Automatic Material Properties Estimation for the Physics-Based Robotic Garment Folding

Vladimír Petrík[1], Jakub Cmíral[1], Vladimír Smutný[1], Pavel Krsek[1], Václav Hlaváč[1]

Abstract— The estimation of the fabric material property during the folding is presented. The available techniques for the accurate garment folding rely on known material properties. Currently, the properties are estimated by an operator in advance of folding. We propose an iterative strategy, which updates the property while the garment is folded. The estimation is formulated as an optimisation task. It is based on measurements from a laser range finder. The proposed algorithm improves the estimation iteratively and prevents the garment from slipping at the same time. We demonstrate the estimation procedure for 10 fabric strips of different materials.

I. INTRODUCTION

One of the core tasks in a robotic garment folding pipeline is the design of the folding path. The execution of the folding path brings the garment from the initially flat state to its folded state. The folding path design is either purely geometrical [1], [2] or is based on the simulation [3], [4]. The geometrical methods require only the size and the position of the garment to be known, but the methods are accurate for specific materials only. The simulation based methods are able to fold a wider range of materials, but rely on the material properties estimation [5]. The state-of-the-art methods estimate the properties manually in advance of the folding. To our knowledge, the automatic estimation of the material properties for the folding purposes has not been addressed yet.

This paper describes the automatic material property called *weight-to-bending-stiffness-ratio* estimation for the physics-based model, which we used for the folding path design in work [3]. The task is motivated by the robotic garment folding but it is simplified to one layer fabrics folding. The estimation is based on the measurements acquired by the 2D laser range finder. It measures the position of the fabric in a single plane cut. The measurement is used to formulate the optimisation problem for the material property estimation. The estimation itself is done in the course of folding. It provides a rough estimation at the beginning of the folding, which is, however, accurate enough to prevent the fabric/garment slipping on the folding desk. The estimation is refined iteratively with new measurements obtained. We demonstrate the proposed estimation procedure using a robotic testbed with the laser range finder (Fig. 1). In a real household scenario, a humanoid robot capable of measuring a point cloud (e.g. PR2 robot) can be used.

[1]Authors are with Czech Institute of Informatics, Robotics, and Cybernetics, Czech Technical University in Prague {vladimir.petrik, jakub.cmiral, vladimir.smutny, pavel.krsek, vaclav.hlavac}@cvut.cz
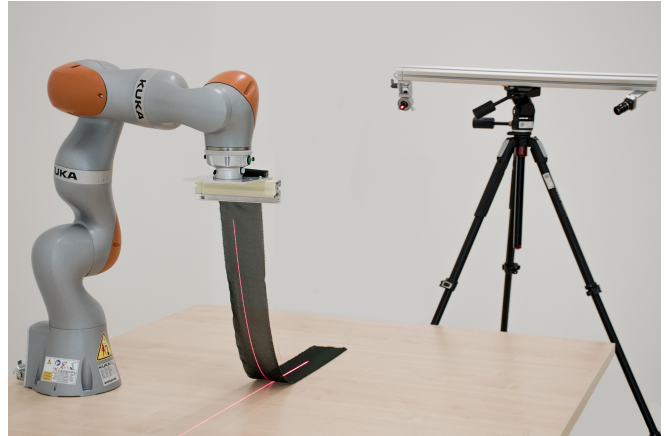
Fig. 1: Robotic testbed used for the demonstration of the proposed algorithm.

The main contribution of the paper is the automatic estimation of the material property in the course of folding. The proposed method replaces the manual estimations performed by an operator before the folding. Using our algorithm, the robotic garment folding can be fully automatic and accurate at the same time.

II. ROBOTIC GARMENT FOLDING

The complete robotic garment folding pipeline was firstly presented for a towel folding in work [6]. It was generalized to more complex garments in works [7], [8]. All works follow the same pipeline, in which the unknown garment is grasped from the pile, it is unfolded while its type is being recognized, and then it is being folded. The unfolding ends with garments laying flat on a folding desk and was studied in works [9], [10], [11], [12], [13], [14]. The folding follows the unfolding and is divided into individual folds as shown in works [15], [16], [17].

Our work studies the folding path design for a single fold. The folding path is either purely geometrical (used in [6], [7]) or simulation-based (used in [8]). Two geometrical paths were proposed: triangular [1] and circular [2]. The triangular path is more suitable for flexible materials and the circular one is more suitable for stiffer materials.

The simulation-based path designs are suitable for wider range of material properties providing an accurate folding result [5]. The first simulation-based path design was proposed in work [18]. The method uses a simplified dynamic model and relies on a dynamically controlled robot. The second path design method [19] uses the simulation software *Maya*.

The last method is based on continuum mechanics and was described separately for one-dimensional fabric models [4] and two-dimensional models [3].

All simulation-based methods assume that the underlying model properties are known or measured in advance of folding. Our goal is to estimate the required properties during folding.

The recently published work [20] represents the underlying model by deep neural network, which was trained in advance of folding by teleoperation. The neural network is used to predict the robot trajectory according to the input image of the scene.

III. FABRIC MODEL

The fabric model in this work is the same as the model used for folding path design in the paper [3]. The model is represented by a Kirchoff-Love shell described in the series of work [21], [22], [23]. The state of the model satisfies the condition of the static equilibrium of forces. The finite element method is used to find the model state following the work [24], which uses isogeometrical analysis described in [25]. The same model was used for the fabric simulation in [26].

Let us denote the fabric model state with a gripper grasping the known part of the fabric (e.g. a corner of a towel) as: $\mathcal{S}(T_g, \eta_m, \eta_b, \nu)$, where T_g is a gripper pose, η_m is *weight-to-membrane-stiffness-ratio*, η_b is *weight-to-bending-stiffness-ratio*, and ν is Poisson's ratio. Parameters η_m, η_b, and ν represent material properties of the fabric [3]. It was shown in [3] that the material properties: mass density ρ, thickness h, Young's modulus E and Poisson's ratio ν are merged into the properties η_m, η_b, and ν. The *weight-to-stiffness-ratios* are expressed as:

$$\eta_m = \left(1 - \nu^2\right)\frac{\rho}{h\,E}, \qquad \eta_b = 12\left(1 - \nu^2\right)\frac{\rho}{h^3\,E}. \qquad (1)$$

These properties are sufficient to describe the fabric, which state is found by the static analysis. The model state is represented by a fabric surface geometry position, i.e. the function $\mathcal{S}(T_g, \eta_m, \eta_b, \nu)$ returns a fabric surface for the given gripper pose and material properties. The fabric surface geometry is represented by NonUniform Rational B-Splines (NURBS) surface as shown in [24].

A. Path Design

The design of the folding path requires the material properties to be known in advance. The path is computed from the sequence of fabric states, which is found as described in [3]. The individual fabric states are constrained by a partially known gripper pose. The unknown pose parameters are computed such that the folding constraints are satisfied. For example, at the beginning of the folding, the gripper z-coordinate is fixed while the rest of the gripper pose is computed such that horizontal force is minimal. It results in a state:

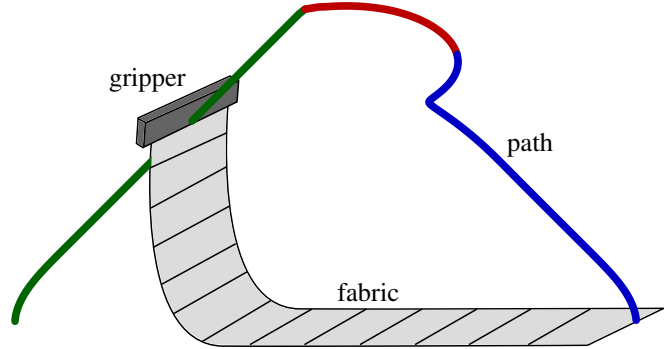$$s_i = \mathcal{S}_1(z_i, \eta_m, \eta_b, \nu), \qquad (2)$$

Fig. 2: The folding path divided into individual phases: *Phase 1* is green, *Phase 2* is red, and *Phase 3* is blue. The fabric model (gray) is divided into elements according to [24].

where z_i represents the gripper pose z-coordinate. The parameter z_i increases monotonically with time resulting in the fabric lifting. The function $\mathcal{S}_1$ represents *Phase 1* in [3]. The *Phase 1* raises the fabric up while keeping the horizontal force minimal. The fabric slipping is avoided by horizontal force minimization.

There are additional two phases, which need to be computed to form the whole folding path. These two phases put the upper layer of the fabric on the fabric lower layer. The constraints in these phases ensure that the upper and lower layer of the folded fabric touch each other in the expected position. The relative position of the upper and lower layer is not changed by the consequent motion. In the *Phase 2*, only the x-coordinate of the gripper pose is known and is increasing monotonically with time. In the last phase, the gripper pose z-coordinate is decreasing monotonically. See [3] for details on the folding path design.

The folding path for the robot is computed from the found sequence of states. We denote the operation of the gripper pose computation from the know state s as:

$$T_g = P(s). \qquad (3)$$

Applying the operator to all states results in the folding path as visualized in Fig. 2.

B. Material Properties Influence

The fabric model depends on three parameters. The first parameter, *weight-to-membrane-stiffness-ratio* η_m, represents the elasticity of the fabric. During the folding, the fabric is stretched by its own weight only. However, typical fabrics are small and exhibit little to none stretch during the folding. For example, the stretch of our 1 m long strips of different materials used in the experiments was less than 3 mm, when stretched by its own weight. We can thus approximate the *weight-to-membrane-stiffness-ratio* by a small value, which represents almost inextensible material. However, the value which is not too small is used to prevent numerical problems. Such an approximation has a negligible influence on the designed folding path.

Poisson's ratio ν represents the amount of material compression in a direction perpendicular to the fabric extension direction. With the small *weight-to-membrane-stiffness-ratio* there is almost none extension, which results in almost none material compression in the perpendicular direction. The influence of Poisson's ratio on the folding is thus negligible too.

The *weight-to-bending-stiffness-ratio* η_b represents the fabric resistance to bending. This is the only property which influences the folding path significantly. It is estimated by the method described in the next section.

IV. PROPERTIES ESTIMATION

The estimation is done during the *Phase 1* of the folding path. As a robot is lifting the fabric, new measurements are obtained and the estimation accuracy is improved.

Different materials require different path for the *Phase 1* as shown in Fig. 3. Our goal is to follow the path which is closest to our current estimation. The value of η_b is updated after each new measurement is obtained. The next gripper position is computed from the updated value of η_b. Without the path updating, the followed path would not corresponds to the path which would be appropriate for the manipulated fabric. It would result in the horizontal force which could cause the fabric slipping.
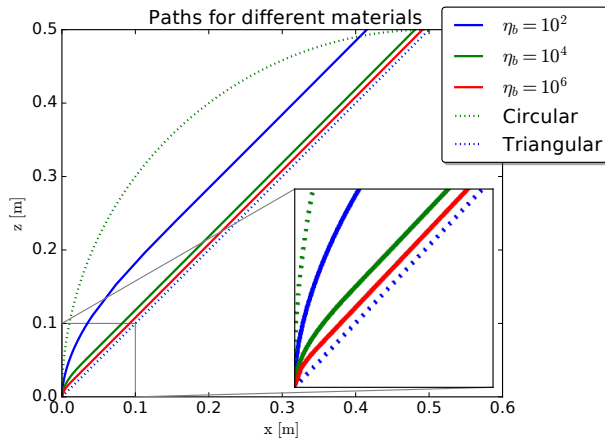

Fig. 3: The paths for different materials. The optimal path in the lower-left corner of the figure lies in between the triangular and circular path depending on the property η_b. Path for the softer material is closer to the triangular path and the stiffer material path is closer to the circular path. The zoom of the lower-left corner is show on the right side.

At the beginning, the fabric is lifted into the gripper pose T_0 computed from the fabric state s_0:

$$s_0 = S_1(z_0,\ \eta_m,\ \eta_b^0,\ \nu), \qquad (4)$$
$$T_0 = P(s_0), \qquad (5)$$

where S_1 represents *Phase 1* and an operator $P(\cdot)$ stands for the gripper pose computation from the fabric state. Properties

Data: $\eta_m,\ \nu,\ \eta_b^0,\ \Delta z_g$
Result: $\eta_b,\ T_\delta$
$T_\delta^0 \leftarrow$ identity
$z_g \leftarrow 0$
for $i \leftarrow 0$ **to** *number of iterations* **do**
    $z_g \leftarrow z_g + \Delta z_g$
    $s_i \leftarrow S_1(z_g,\ \eta_m,\ \eta_b^i,\ \nu)$
    $T_i \leftarrow P(s_i)$
    move robot to pose T_i
    $Z_i \leftarrow$ obtain a new measurement
    $\eta_b^{i+1}, T_\delta^{i+1} \leftarrow \underset{\eta_b, T_\delta}{\arg\min}\, J(T_i, Z_i, \eta_b, T_\delta)$
end
Algorithm 1: Iterative material property estimation

η_m and ν are constant. The value η_b^0 is an initial guess for the *weight-to-bending-stiffness-ratio*. For the initial guess we use small value which represents a path which is close to the circular path. We observed that the circular path does not result in the fabric slipping at the beginning of the folding motion. In the later part of the folding motion the gripper follows the path corresponding to the estimated η_b value.()

After the robot reaches the computed pose T_0, the new measurement of the fabric shape Z_0 is obtained. The estimation assumes the measurement in form of the point cloud consisting of points: $z_i,\ i = 1, \ldots, N$. Based on the measurement, the new value for η_b is estimated:

$$\eta_b^1 = \arg\min_{\eta_b} J(T_0, Z_0, \eta_b), \qquad (6)$$

where $J(\cdot, \cdot, \cdot)$ is a cost function defined as:

$$J(T, Z, \eta_b) = \frac{1}{2} \sum_{z \in Z} d(z, S(T, \eta_m, \eta_b, \nu))^2, \qquad (7)$$

with a function $d(z, S(\cdot))$ representing the Euclidean distance between the fabric surface and measured point. In our implementation, the position of the NURBS surface was evaluated on a fine rectangular grid, and the closest position was used. The new gripper pose T_1 is obtained with the estimated η_b^1 following Eq. (4, 5). The process continues iteratively during the whole *Phase 1*.

The presented estimation process requires the gripper position to be known precisely. In practice, this is however unfeasible due to the overall robotic testbed accuracy. In order to make the estimation process feasible in the presence of this uncertainty, we relaxed the constraints by adding an unknown gripper position offset into the optimisation process. This changes the cost function (7) into:

$$J(T, Z, \eta_b, T_\delta) = \frac{1}{2} \sum_{z \in Z} d(z, S(TT_\delta, \eta_m, \eta_b^0, \nu))^2, \quad (8)$$

where T_δ represents the unknown translation matrix. The properties being estimated are thus: η_b and T_δ. The complete algorithm for iterative parameters estimation is shown in listing 1.

V. EXPERIMENTS

A. Testbed Description

A single-arm robot *KUKA LBR iiwa 7* was used for the fabric manipulation purposes. For the point cloud measurement, we used a monocular camera and laser plane projector. The robot, camera and projector were calibrated to each other. It allows us to measure the fabric shape in the projected plane. The real testbed and the schematic visualisation are shown in Fig. 1 and Fig. 4.
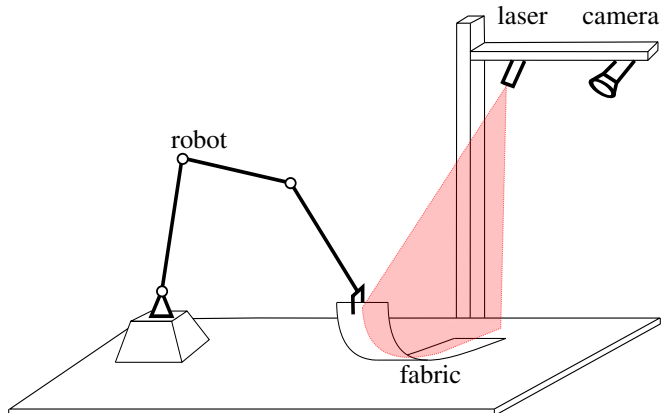

Fig. 4: Schematic visualisation of the robotic testbed. The robot, laser plane projector, and camera are calibrated with respect to each other. It allows us to measure the fabric surface shape.

B. Manual Reference Properties Measurement

To verify the estimation algorithm, we used narrow fabric strips of different materials. We used single layer materials from the whole spectrum of weaving fabrics used for fabric manufacturing. The reference strips *weight-to-bending-stiffness-ratio* are not known a priori. To estimate them, we used manual measurements of the folded fabric height h_m as shown in Fig. 5. This process of estimation is called a free fold test as described in [27]. The relation between η_b and h_m is shown in Fig. 6 and we denote the ratio computation as: $\eta_b = \eta_b(h_m)$.

Fig. 5: Free fold test is an offline method of the *weight-to-bending-stiffness-ratio* estimation.

Besides the material properties used in our model, properties, which reflect the history of the particular patch of the fabric such as ironing, washing, bending, storing conditions, moisture content influence the actual bending shape during folding. Therefore, we measure the height multiple times with different free fold test locations and we estimate the reference ratio in a statistical manner. Measured values h_m together with an estimated mean μ_h and $\pm 2\sigma_h$, where σ_h
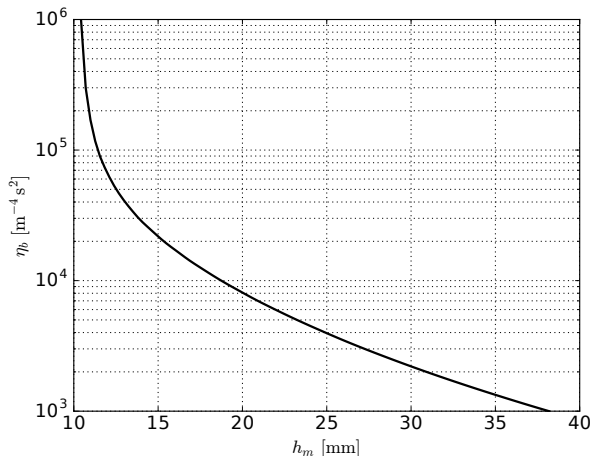

Fig. 6: The *weight-to-bending-stiffness-ratio* η_b as a function of the measured height h_m.

stands for standard deviation, are shown in Fig. 7. We visualize the material property uncertainty with the 4σ interval. From the estimated height statistical values μ_h and σ_h, the expected values of η_b are computed as shown in Tab. I and Fig. 8.

TABLE I: Reference material properties.

Material	μ_h [mm]	$2\sigma_h$ [mm]	$\eta_b(\mu_h)$ [m^{-4}s^2]	$\eta_b(\mu_h \pm 2\sigma_h)$ [m^{-4}s^2]
coating	20	3.4	$8.5 \cdot 10^3$	$5.1 \cdot 10^3$ - $1.6 \cdot 10^4$
chanel	28	3.9	$2.6 \cdot 10^3$	$1.7 \cdot 10^3$ - $4.2 \cdot 10^3$
twill	19	4.6	$8.9 \cdot 10^3$	$4.5 \cdot 10^3$ - $2.3 \cdot 10^4$
denim	23	3.1	$5.2 \cdot 10^3$	$3.4 \cdot 10^3$ - $8.3 \cdot 10^3$
terry cloth	25	2.8	$3.9 \cdot 10^3$	$2.8 \cdot 10^3$ - $5.7 \cdot 10^3$
plain weave	25	3.4	$4.0 \cdot 10^3$	$2.7 \cdot 10^3$ - $6.4 \cdot 10^3$
herringbone	21	2.5	$6.5 \cdot 10^3$	$4.6 \cdot 10^3$ - $9.7 \cdot 10^3$
georgette	15	1.7	$2.4 \cdot 10^4$	$1.6 \cdot 10^4$ - $4.1 \cdot 10^4$
chiffon	13	2.3	$3.5 \cdot 10^4$	$1.8 \cdot 10^4$ - $1.5 \cdot 10^5$
wool suiting	18	1.8	$1.1 \cdot 10^4$	$8.0 \cdot 10^3$ - $1.5 \cdot 10^4$

C. Strips Properties Estimation

We have observed, that the η_b value for the wide range of materials lies in a range from 10^2 to 10^6 m^{-4}s^2. We chose an initial guess for the estimated value to be $\eta_b^0 = 10^2$ m^{-4}s^2. The initial guess value does not seem to influence the resulting estimate. The value of η_b is then updated iteratively following Algorithm 1. The whole *Phase 1* is used, and we divided it into 10 iterations. The values estimated in the last iteration for all tested materials are shown in Fig. 8. The path followed by the gripper and the reference path for the selected fabric are shown in Fig. 9. The estimations for all tested fabrics are shown in Fig. 10.

The results shown in Fig. 10 indicate that the estimation is improved as the fabric is lifted. The initial rough estimation was however sufficient to prevent the fabric from slipping. Estimated values have much lower uncertainty than the interval of values which prevent the slipping as shown in [4]. We did not observe any slipping during the whole
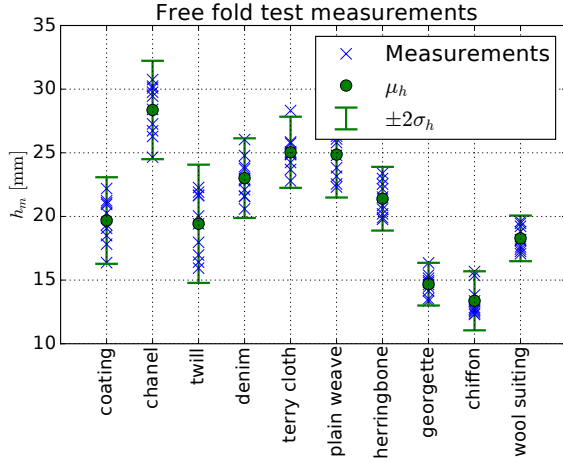
Fig. 7: Measurements for the free fold test. The mean value and standard deviation is computed from the height measurements.
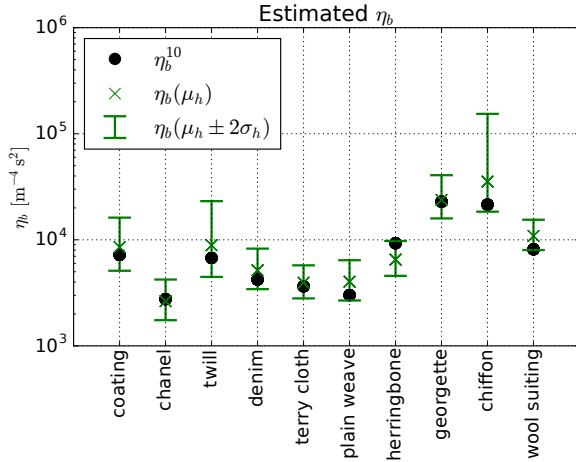

Fig. 8: The reference η_b estimated by the free fold test (green cross) and the value estimated in the last iteration of the proposed algorithm (black dot). The visualized range represents uncertainty of reference value estimation.

experiment. The value estimated in the last iteration (Fig. 8) for all materials was in a range of $\pm 2\sigma_h$.

VI. CONCLUSIONS

We have presented the algorithm for estimation of the material property for the robotic garment folding purposes. The estimation is done iteratively in the course of folding while updating the folding path. The formulated optimisation task uses the measurement of the fabric shape, provided in the form of a point cloud. It replaces the state-of-the-art estimation technique, which was done manually by an operator.

We demonstrated the accuracy of our approach experimentally using the robotic testbed with the laser range finder. The 1 m long fabric strips of various materials were tested.
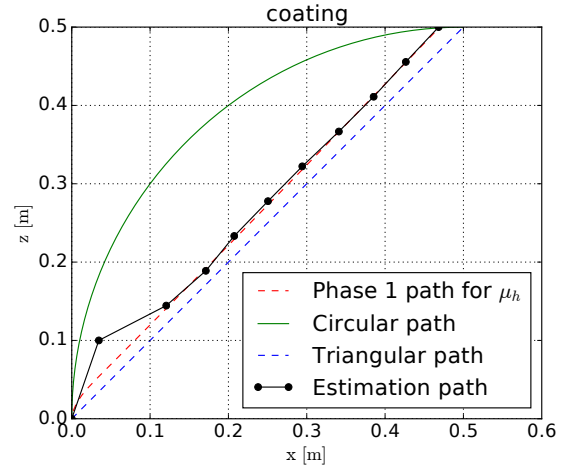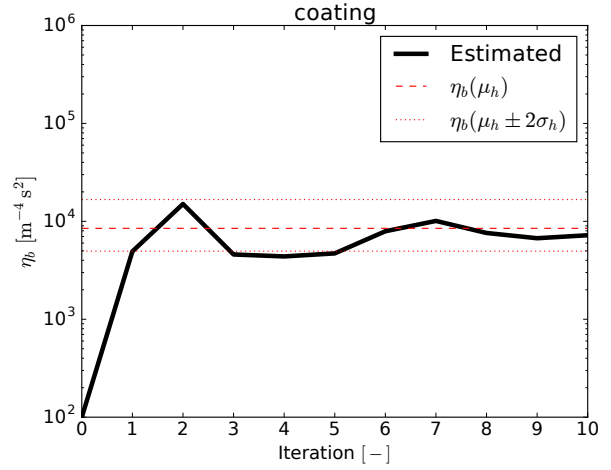

Fig. 9: The iterative update of the *weight-to-bending-stiffness-ratio* and the gripper position for the selected fabric. The red dashed line represents the reference values estimated from the free fold test. The uncertainty of the estimation is represented by red dotted lines. The triangular (blue, dashed) and circular (green) paths are shown as a reference.

So far we have tested the estimation algorithm on one-layer samples only since they satisfy the assumptions of the fabric model. In future work, the limits of the model, as well as the limits of the estimation algorithm, should be tested on multi-layer fabrics as well as other technical materials such as rubber strips, steel sheets, etc.

REFERENCES

[1] J. van den Berg, S. Miller, K. Y. Goldberg, and P. Abbeel, "Gravity-based robotic cloth folding." in *Int. Workshop on the Algorithmic Foundations of Robotics (WAFR)*, 2010, pp. 409–424.
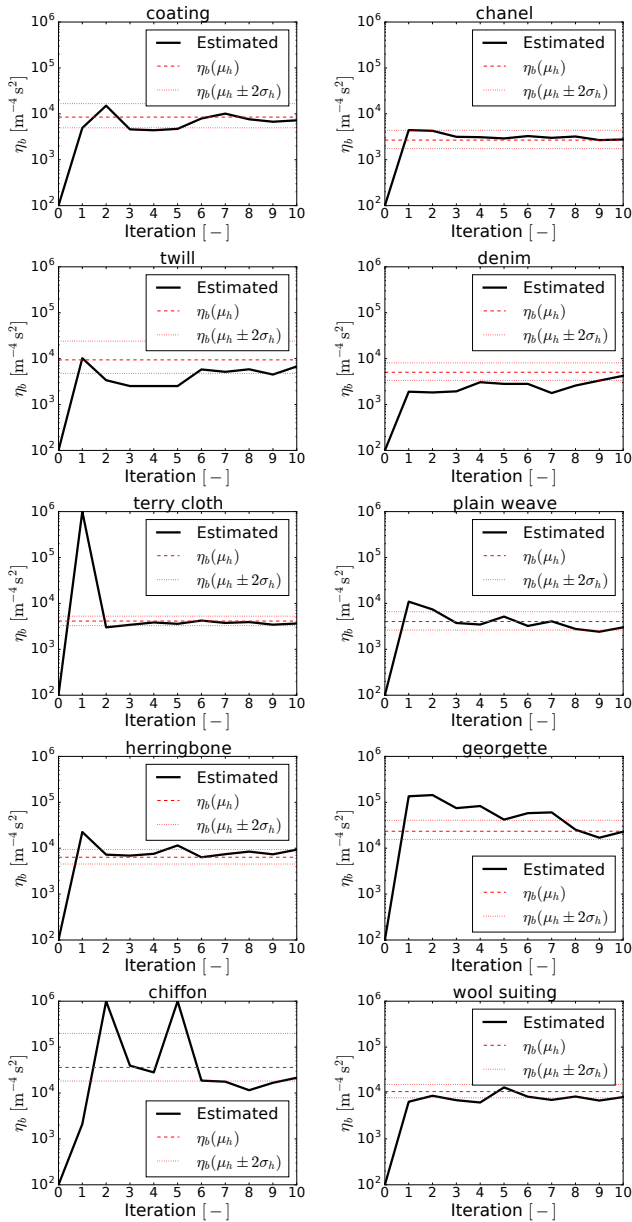
Fig. 10: The iterative estimation of η_b for all tested materials.

[2] V. Petrík, V. Smutný, P. Krsek, and V. Hlaváč, "Robotic Garment Folding: Precision Improvement and Workspace Enlargement," in *Annu. Conf. Towards Autonomous Robotic Systems (TAROS)*, Liverpool, 2015, pp. 204–215.

[3] V. Petrík, V. Smutný, P. Krsek, and V. Hlaváč, "Single arm robotic garment folding path generation," *Advanced Robotics*, vol. 31, no. 24-24, pp. 1325–1337, 2017. [Online]. Available: http://dx.doi.org/10.1080/01691864.2017.1367325

[4] V. Petrík, V. Smutný, P. Krsek, and V. Hlaváč, "Physics-Based Model of Rectangular Garment for Robotic Folding," in *Proc. Int. Conf. on Intelligent Robots and Systems (IROS)*, Daejeon, 2016, pp. 951–956.

[5] ——, "Accuracy of Robotic Elastic Object Manipulation as a Function of Material Properties," in *Int. Workshop on Modelling and Simulation for Autonomous Systems (MESAS)*, Rome, 2016, pp. 384–395.

[6] J. Maitin-Shepard, M. Cusumano-Towner, J. Lei, and P. Abbeel, "Cloth grasp point detection based on multiple-view geometric cues with application to robotic towel folding," in *Proc. IEEE Int. Conf. on Robotics and Automation (ICRA)*, 2010, pp. 2308–2315.

[7] A. Doumanoglou, J. Stria, G. Peleka, I. Mariolis, V. Petrík, A. Kargakos, L. Wagner, V. Hlaváč, T.-K. Kim, and S. Malassiotis, "Folding clothes autonomously: A complete pipeline," *IEEE Transactions on Robotics*, 2016.

[8] Y. Li, Y. Wang, Y. Yue, D. Xu, M. Case, S.-F. Chang, E. Grinspun, and P. Allen, "Model-driven feed-forward prediction for manipulation of deformable objects," *arXiv preprint arXiv:1607.04411*, 2016.

[9] H. Yuba, S. Arnold, and K. Yamazaki, "Unfolding of a rectangular cloth from unarranged starting shapes by a dual-armed robot with a mechanism for managing recognition error and uncertainty," *Advanced Robotics*, vol. 31, no. 10, pp. 544–556, 2017.

[10] Y. Li, D. Xu, Y. Yue, Y. Wang, S.-F. Chang, E. Grinspun, and P. K. Allen, "Regrasping and unfolding of garments using predictive thin shell modeling," in *Proc. IEEE Int. Conf. on Robotics and Automation (ICRA)*, 2015, pp. 1382–1388.

[11] M. Cusumano-Towner, A. Singh, S. Miller, J. F. O'Brien, and P. Abbeel, "Bringing clothing into desired configurations with limited perception," in *Proc. IEEE Int. Conf. on Robotics and Automation (ICRA)*, 2011, pp. 3893–3900.

[12] A. Doumanoglou, A. Kargakos, T.-K. Kimand, and S. Malassiotis, "Autonomous active recognition and unfolding of clothes using random decision forests and probabilistic planning," in *Proc. IEEE Int. Conf. on Robotics and Automation (ICRA)*, 2014, pp. 987–993.

[13] D. Triantafyllou, I. Mariolis, A. Kargakos, S. Malassiotis, and N. Aspragathos, "A geometric approach to robotic unfolding of garments," *Robotics and Autonomous Systems*, vol. 75, pp. 233 – 243, 2016.

[14] F. Osawa, H. Seki, and Y. Kamiya, "Unfolding of massive laundry and classification types by dual manipulator." *J. Advanced and Intelligent Informatics (JACIII)*, vol. 11, no. 5, pp. 457–463, 2007.

[15] S. Miller, J. van den Berg, M. Fritz, T. Darrell, K. Goldberg, and P. Abbeel, "A geometric approach to robotic laundry folding," *Int. J. Robotics Research (IJRR)*, vol. 31, no. 2, pp. 249–267, 2012.

[16] S. Miller, M. Fritz, T. Darrell, and P. Abbeel, "Parametrized shape models for clothing," in *Proc. IEEE Int. Conf. on Robotics and Automation (ICRA)*, 2011, pp. 4861–4868.

[17] J. Stria, D. Průša, V. Hlaváč, L. Wagner, V. Petrík, P. Krsek, and V. Smutný, "Garment perception and its folding using a dual-arm robot," in *Proc. Int. Conf. on Intelligent Robots and Systems (IROS)*, Chicago, Illinois, 2014, pp. 61–67.

[18] Y. Yamakawa, A. Namiki, and M. Ishikawa, "Motion planning for dynamic folding of a cloth with two high-speed robot hands and two high-speed sliders," in *Robotics and Automation (ICRA), 2011 IEEE International Conference on*. IEEE, 2011, pp. 5486–5491.

[19] Y. Li, Y. Yue, D. Xu, E. Grinspun, and P. K. Allen, "Folding deformable objects using predictive simulation and trajectory optimization," in *Proc. Int. Conf. on Intelligent Robots and Systems (IROS)*, 2015, pp. 6000–6006.

[20] P. C. Yang, K. Sasaki, K. Suzuki, K. Kase, S. Sugano, and T. Ogata, "Repeatable folding task by humanoid robot worker using deep learning," *IEEE Robotics and Automation Letters*, vol. 2, no. 2, pp. 397–403, April 2017.

[21] J. C. Simo, D. D. Fox, and M. S. Rifai, "On a stress resultant geometrically exact shell model. Part III: computational aspects of the nonlinear theory," *Computer Methods in Applied Mechanics and Engineering*, vol. 79, no. 1, pp. 21–70, 1990.

[22] ——, "On a stress resultant geometrically exact shell model. Part II: the linear theory; computational aspects," *Computer Methods in Applied Mechanics and Engineering*, vol. 73, no. 1, pp. 53–92, 1989.

[23] J. C. Simo and D. D. Fox, "On a stress resultant geometrically exact shell model. Part I: formulation and optimal parametrization," *Computer Methods in Applied Mechanics and Engineering*, vol. 72, no. 3, pp. 267–304, 1989.

[24] J. Kiendl, K.-U. Bletzinger, J. Linhard, and R. Wüchner, "Isogeometric shell analysis with Kirchhoff–Love elements," *Computer Methods in Applied Mechanics and Engineering*, vol. 198, no. 49, pp. 3902–3914, 2009.

[25] T. J. Hughes, J. A. Cottrell, and Y. Bazilevs, "Isogeometric analysis: CAD, finite elements, NURBS, exact geometry and mesh refinement," *Computer methods in applied mechanics and engineering*, vol. 194, no. 39, pp. 4135–4195, 2005.

[26] J. Lu and C. Zheng, "Dynamic cloth simulation by isogeometric analysis," *Computer Methods in Applied Mechanics and Engineering*, vol. 268, pp. 475 – 493, Jan. 2014.

[27] R. H. Plaut, "Formulas to determine fabric bending rigidity from simple tests," *Textile Research Journal*, vol. 85, no. 8, pp. 884–894, 2015.